On the implementation of finite strain plasticity equations in a numerical model

37. Laun, H. M., 'Elstische Deformationsanteile bei der Dehnung und Scherung von Kunststoffschemelzen', Jahrestagung Deutsche Rheol. Gesellschaft, Aachen (1979).
38. Middleman, S., *Fundamentals of Polymer Processing*, McGraw-Hill, New York (1977).
39. Bird, R. B., Armstrong, R. C., and Hassager, O., *Dynamics of Polymeric Liquids*, Vol. 1., *Fluid Mechanics*, p. 50 John Wiley & Sons (1977).
40. White, J. L., and Huang, D., 'Extrudate Swell and Extrusion Pressure Loss of Polymer Melts Flowing Through Rectangular and Trapezoidal Dies', *Patra Report* No. 166 (1981).

Numerical Analysis of Forming Processes
Edited by J. F. T. Pittman, O. C. Zienkiewicz, R. D. Wood, and J. M. Alexander

Chapter 12

On the Implementation of Finite Strain Plasticity Equations in a Numerical model

Joop C. Nagtegaal and Frans E. Veldpaus

12.1 INTRODUCTION

In the finite element analysis of metal-forming problems, one faces a number of difficulties which at first sight seem to preclude the development of an efficient solution procedure.

1. The material satisfies a constitutive rate equation, which can be of complicated form and may change considerably during plastic straining.
2. The rate of stress used in the constitutive equation is not an ordinary rate, but a co-rotational (Jaumann) rate.
3. The constitutive rate equation is formulated with respect to the current state of the material at any time.
4. Analysis up to large strains is desired.
5. Large material rotations may occur at any time.

The first three aspects of metal-forming analysis mentioned above seem to require an analysis procedure in which small deformation increments are taken in order to get sufficient accuracy. The last two aspects, however, demand that in an efficient solution procedure large strains and rotations can be obtained in a minimum number of increments.

From the earlier work on the subject of metal-forming analysis, two different approaches have emerged: the 'flow' approach and the 'solid' approach. In the 'flow' approach, the metal is considered to behave as a non-Newtonian fluid, and the finite element equations are solved accordingly. With this approach, which was amongst others propagated by the Swansea group,[1,2] one can achieve quite large increments in strain and rotation, and hence obtain effective solutions to many metal-forming problems. However, many of the subtleties of the elastic–plastic constitutive equations are not taken into account, which has made 'plasticians' worried about the correctness of the 'flow' assumptions. Also, the method in its original form does not yield the residual stresses, which are often desired as a result of finite element analysis.

In the 'solid' approach, the material is considered to behave as a (classical) elastic–plastic solid, and the finite element equations are solved with methods used in small-strain plasticity problems. Various continuum mechanics formulations were originally proposed for the metal-forming problem. The 'updated Lagrange' method, first precisely defined by McMeeking and Rice,[3] now forms the basis for most work on the subject. With the 'solid' approach the constitutive equations can be handled concisely. However, in its original form severe limitations exist as to the magnitude of strain and rotation increments, which makes the method rather expensive.

Over the years, substantial improvements have been made to both methods. The 'flow' approach has been extended to deal with such phenomena as residual stresses and work hardening,[4] whereas the 'solid' approach has been improved so that it can deal with large rotation increments.[5]

In this paper we attempt to extend the 'solid' approach further so that it is also able to handle large strain increments. This is not the first paper which attempts to make this extension. Hughes *et al.*, in a paper on three-dimensional shells (!),[6] propose a simple method to calculate finite rotation and strain increments from a given displacement increment. The method uses the classical linear expression for deformation rate and spin, but taken in the state at the middle of the displacement increment. Hughes, however, does not discuss how the resulting nonlinear equations should be solved.

In a recent paper by Nagtegaal,[7] another method is proposed to deal with large strain and rotation increments. In this method, the assumption of a straight strain path was introduced to calculate an approximate average strain rate from a given displacement increment, and the Newton–Raphson method is used to solve the resulting nonlinear equations. The method is quite effective, but requires the use of a variety of stress and strain measures and rather cumbersome transformations between them, which makes it not very appealing.

In the current paper the above method is cast in a more natural form. First the constitutive rate equation is integrated to incremental form. This requires introduction of so-called 'rotation-neutralized' stresses, moduli, deformation rates and of the single assumption that the rotation-neutralized deformation rate is constant. With the integrated constitutive equations, a set of incremental nonlinear governing equations can be formulated, which must be solved by an iterative method. The Newton–Raphson method is used as solution procedure, and this requires linearization of the governing equations around the last obtained state. It is highly remarkable that this linearized form is equal to the rate form used by McMeeking and Rice,[3] with the only difference being that the elastic plastic rate moduli used by the latter authors are replaced by the moduli, giving the relation between change in stress increment and change in strain increment. A simple approximate integration procedure is used to derive these moduli.

It is shown in a number of examples that the method developed in this paper forms an effective tool for the analysis of metal-forming problems. Large increments can be taken without significant loss of accuracy. The only problem still observed is the lack of convergence of the Newton–Raphson method if the increment size increases over a certain (problem-dependent) value. This problem would presumably be overcome with use of a more stable iterative procedure: however, it would not necessitate modification of the governing equations.

12.2 AN INTEGRATED FORM OF THE CONSTITUTIVE RATE EQUATIONS

The generally accepted constitutive rate equation in finite strain plasticity calculations is:

$$\overset{\nabla}{\boldsymbol{\sigma}} = \dot{\boldsymbol{\sigma}} + \boldsymbol{\Omega}^{\mathrm{T}}\cdot\boldsymbol{\sigma} + \boldsymbol{\sigma}\cdot\boldsymbol{\Omega} = \mathbf{L}:\mathbf{D} \tag{12.1}$$

where $\overset{\nabla}{\boldsymbol{\sigma}}$ is the Jaumann rate of the Cauchy stress tensor $\boldsymbol{\sigma}$, $\boldsymbol{\Omega}$ is the spin tensor, $\mathbf{D}$ is the deformation rate tensor and $\mathbf{L}$ is the fourth-order tensor of moduli. $\mathbf{D}$ and $\boldsymbol{\Omega}$ are related to the deformation tensor $\mathbf{F}$ by:

$$\mathbf{D} + \boldsymbol{\Omega} = \dot{\mathbf{F}}\cdot\mathbf{F}^{-1}; \quad \mathbf{D} = \mathbf{D}^{\mathrm{T}}; \quad \boldsymbol{\Omega} = -\boldsymbol{\Omega}^{\mathrm{T}} \tag{12.2}$$

In order to integrate the rate Equation (12.1) to incremental form we introduce the orthogonal tensor $\boldsymbol{\rho}$, describing the rotation of the material with respect to the configuration at the beginning of the increment, i.e. at time $t = t_0$. This rotation tensor describes the transformation of any unit vector $\mathbf{N}$ at $t = t_0$ to a unit vector $\mathbf{n}$ at the current time:

$$\mathbf{n} = \boldsymbol{\rho}\cdot\mathbf{N} \tag{12.3}$$

Differentiation of this relation with respect to time yields

$$\dot{\mathbf{n}} = \dot{\boldsymbol{\rho}}\cdot\mathbf{N} \tag{12.4}$$

On the other hand, the spin tensor yields for the rate of change of $\mathbf{n}$

$$\dot{\mathbf{n}} = \boldsymbol{\Omega}\cdot\mathbf{n} \tag{12.5}$$

Combination of Equations (12.3), (12.4) and (12.5) then yields that $\boldsymbol{\rho}$ satisfies the differential equation

$$\dot{\boldsymbol{\rho}} = \boldsymbol{\Omega}\cdot\boldsymbol{\rho} \qquad \text{for} \qquad t > t_0 \tag{12.6}$$

with the initial condition that $\boldsymbol{\rho}$ is equal to the unit tensor $\mathbf{I}$ at time t_0. The tensor $\boldsymbol{\rho}$ can be used to define the so-called rotation-neutralized quantities $\bar{\mathbf{F}}$, $\bar{\boldsymbol{\Omega}}$, $\bar{\mathbf{D}}$, $\bar{\boldsymbol{\sigma}}$ and $\bar{\mathbf{L}}$:

$$\bar{\mathbf{F}} = \boldsymbol{\rho}^{\mathrm{T}}\cdot\mathbf{F} \tag{12.7a}$$

$$\bar{\boldsymbol{\Omega}} = \boldsymbol{\rho}^{\mathrm{T}}\cdot\boldsymbol{\Omega}\cdot\boldsymbol{\rho} \tag{12.7b}$$

$$\bar{\mathbf{D}} = \boldsymbol{\rho}^{\mathrm{T}}\cdot\mathbf{D}\cdot\boldsymbol{\rho} \tag{12.7c}$$

$$\bar{\boldsymbol{\sigma}} = \boldsymbol{\rho}^{\mathrm{T}}\cdot\boldsymbol{\sigma}\cdot\boldsymbol{\rho} \tag{12.7d}$$

$$\bar{\mathbf{L}} = \boldsymbol{\rho}^{\mathrm{T}}\cdot[\boldsymbol{\rho}^{\mathrm{T}}\cdot\mathbf{L}\cdot\boldsymbol{\rho}]\cdot\boldsymbol{\rho} \tag{12.7e}$$

If the material is inherently isotropic, i.e. if any anisotropy will only depend on the development of $\boldsymbol{\sigma}$ and perhaps on other tensor quantities $\boldsymbol{\alpha}_i$, we may consider $\mathbf{L}$ as a function of $\boldsymbol{\sigma}$ and $\boldsymbol{\alpha}_i$ and hence we may write

$$\bar{\mathbf{L}}(\boldsymbol{\sigma}, \boldsymbol{\alpha}_i) = \mathbf{L}(\bar{\boldsymbol{\sigma}}, \bar{\boldsymbol{\alpha}}_i) \tag{12.8}$$

Differentiation of Equation (12.7d) with respect to time yields

$$\begin{aligned}\dot{\bar{\boldsymbol{\sigma}}} &= \boldsymbol{\rho}^{\mathrm{T}}\cdot\dot{\boldsymbol{\sigma}}\cdot\boldsymbol{\rho} + \dot{\boldsymbol{\rho}}^{\mathrm{T}}\cdot\boldsymbol{\sigma}\cdot\boldsymbol{\rho} + \boldsymbol{\rho}^{\mathrm{T}}\cdot\boldsymbol{\sigma}\cdot\dot{\boldsymbol{\rho}} \\ &= \boldsymbol{\rho}^{\mathrm{T}}\cdot(\dot{\boldsymbol{\sigma}} + \boldsymbol{\Omega}^{\mathrm{T}}\cdot\boldsymbol{\sigma} + \boldsymbol{\sigma}\cdot\boldsymbol{\Omega})\cdot\boldsymbol{\rho} = \boldsymbol{\rho}^{\mathrm{T}}.\overset{\nabla}{\boldsymbol{\sigma}}\cdot\boldsymbol{\rho}\end{aligned} \tag{12.9}$$

Formulated in rotation-neutralized quantities, the constitutive rate Equation (12.1) can hence be written as

$$\dot{\bar{\boldsymbol{\sigma}}} = \bar{\mathbf{L}}:\bar{\mathbf{D}}; \qquad \bar{\boldsymbol{\sigma}}(t_0) = \boldsymbol{\sigma}(t_0) = \boldsymbol{\sigma}_0 \tag{12.10}$$

This equation with the given initial condition can now be integrated to incremental form. For the stress tensor $\bar{\boldsymbol{\sigma}}_e = \bar{\boldsymbol{\sigma}}(t_e)$ at the end of the increment, i.e. at time $t = t_e = t_0 + \Delta t$, we find

$$\bar{\boldsymbol{\sigma}}_e = \boldsymbol{\sigma}_0 + \Delta\bar{\boldsymbol{\sigma}}; \qquad \Delta\bar{\boldsymbol{\sigma}} = \int_{t_0}^{t_e} \bar{\mathbf{L}}:\bar{\mathbf{D}}\,\mathrm{d}t \tag{12.11}$$

All relations derived so far are exact for any deformation path. A further evaluation of Equation (12.11) requires an assumption about this path. We assume that the rotation-neutralized deformation rate tensor $\bar{\mathbf{D}}$ is constant in the increment and equal to $(1/\Delta t)\bar{\mathbf{C}}$. Elimination of $\mathbf{D}$ and $\mathbf{F}$ from Equations (12.2), (12.7a) and (12.7c) then yields the relation

$$\bar{\mathbf{D}} = \dot{\bar{\mathbf{F}}}\cdot\bar{\mathbf{F}}^{-1} = \frac{1}{\Delta t}\bar{\mathbf{C}}; \qquad \bar{\mathbf{C}} = \bar{\mathbf{C}}^{\mathrm{T}},\text{ constant.} \tag{12.12}$$

The solution of this differential equation with the initial condition $\bar{\mathbf{F}}(t_0) = \mathbf{F}(t_0) = \mathbf{I}$ is

$$\bar{\mathbf{F}} = \bar{\mathbf{F}}^{-\mathrm{T}} = \exp\left(\frac{t-t_0}{\Delta t}\bar{\mathbf{C}}\right) \qquad \text{for} \qquad t_0 \leqslant t \leqslant t_e \tag{12.13}$$

The calculation of exponential and logarithmic functions of symmetric tensors is discussed in Appendix 12A. Hence with the assumed deformation path the tensor $\bar{\mathbf{F}}$ will be symmetric. From $\bar{\mathbf{F}}^{\mathrm{T}}\cdot\bar{\mathbf{F}} = \mathbf{F}^{\mathrm{T}}\cdot\mathbf{F}$ and the polar decomposition $\mathbf{F} = \mathbf{R}\cdot\mathbf{U}$, it then follows that $\bar{\mathbf{F}}$ is equal to the symmetrical deformation tensor $\mathbf{U}$ while $\boldsymbol{\rho}$ equals the rotation tensor $\mathbf{R}$

$$\mathbf{F} = \mathbf{R}\cdot\mathbf{U}; \quad \bar{\mathbf{F}} = \mathbf{U} = (\mathbf{F}^{\mathrm{T}}\cdot\mathbf{F})^{1/2}; \quad \boldsymbol{\rho} = \mathbf{R} = \mathbf{F}\cdot\mathbf{U}^{-1} \tag{12.14}$$

Replacing t in Equation (12.13) by $t_e = t_0 + \Delta t$ and solving for $\bar{\mathbf{C}}_e$ leaves us with the desired relation between $\bar{\mathbf{C}}_e = \Delta t\bar{\mathbf{D}}$ and $\mathbf{F}_e$

$$\bar{\mathbf{C}}_e = \ln(\mathbf{U}_e) = \tfrac{1}{2}\ln(\mathbf{F}_e^{\mathrm{T}}\cdot\mathbf{F}_e) \tag{12.15}$$

Using Equation (12.12), the rotation neutralized stress tensor $\boldsymbol{\sigma}_e$ is found to be

$$\bar{\boldsymbol{\sigma}}_e = \boldsymbol{\sigma}_0 + \Delta\bar{\boldsymbol{\sigma}}; \qquad \Delta\bar{\boldsymbol{\sigma}} = \left[\frac{1}{\Delta t}\int_{t_0}^{t_e} \bar{\mathbf{L}}\,\mathrm{d}t\right]:\bar{\mathbf{C}}_e \tag{12.16}$$

The Cauchy stress $\boldsymbol{\sigma}_e = \boldsymbol{\sigma}(t_e)$ at the end of the increment now follows from

$$\boldsymbol{\sigma}_e = \mathbf{R}_e\cdot\bar{\boldsymbol{\sigma}}_e\cdot\mathbf{R}_e^{\mathrm{T}} \tag{12.17}$$

The assumed constant deformation rate is in general an approximation to the actual deformation rate. The magnitude of the error depends on the nature of the deformation. For uniaxial tension, the error is essentially zero, and hence no accuracy limit exists for the size of the strain increment. In other cases, however, the error increases with the size of the increment. As an example, approximate and actual deformation rates are calculated for an increment in simple shear in Appendix 12B.

12.3 VARIATIONAL FORMULATION AND SOLUTION PROCEDURE

To formulate equilibrium at the end of the increment, the principle of virtual work is used. Denoting the quantity $\phi(t)$ at time $t = t_e = t_0 + \Delta t$, that is, $\phi(t_e)$ as ϕ (no subscript is used for brevity of the notation), the virtual work equation at time $t = t_e$ is given by

$$\int_V \boldsymbol{\sigma}:\delta\boldsymbol{\varepsilon}\,\delta V = \int_V \mathbf{q}\cdot\delta\mathbf{u}\,\mathrm{d}V + \int_S \mathbf{p}\cdot\delta\mathbf{u}\,\mathrm{d}S \tag{12.18}$$

Here, $\delta\mathbf{u}$ is an arbitrary variation in the displacement field, $\mathbf{q}$ is the volume load and $\mathbf{p}$ is the surface load on the surface S of V. Note that $V = V(t_e)$ and $S = S(t_e)$ are the volume and surface at the end of the increment or at the last obtained approximation for the end of the increment. With use of the gradient operator $\boldsymbol{\nabla}$, the variations in strain in this equation are defined by

$$\delta\boldsymbol{\varepsilon} = \tfrac{1}{2}[(\boldsymbol{\nabla}\,\delta\mathbf{u}) + (\boldsymbol{\nabla}\,\delta\mathbf{u})^{\mathrm{T}}] \tag{12.19}$$

After substitution of $\boldsymbol{\sigma}$ as obtained in the previous section, the equilibrium can be verified.

In order to solve this set of nonlinear equations, an iterative technique must be used. The most commonly used iterative techniques are variants of the Newton–Raphson method, which require linearization of Equation (12.18) around the last obtained solution $\mathbf{u}$. The derivation of this linearized form, which is presented in Appendix 12C, is rather lengthly but otherwise straightforward. If we use a notation in which $d\phi$ is a small change from the last obtained value, this leads to the variational statement

$$\int_V \{d^J\boldsymbol{\sigma}:\delta\boldsymbol{\varepsilon} - 2(d\boldsymbol{\varepsilon}\cdot\boldsymbol{\sigma}):\delta\boldsymbol{\varepsilon} + \operatorname{tr}(d\boldsymbol{\varepsilon})\boldsymbol{\sigma}:\delta\boldsymbol{\varepsilon} + \boldsymbol{\sigma}:[(\nabla d\mathbf{u})\cdot(\nabla\delta\mathbf{u})^T]\}dV$$

$$= d\int_V \mathbf{q}\cdot\delta\mathbf{u}\,dV + d\int_S \mathbf{p}\cdot\delta\mathbf{u}\,dS \qquad (12.20)$$

where the integrations are carried out in the last obtained state. In this statement, which was first derived by Hill,[8] the change in the strain tensor $d\boldsymbol{\varepsilon}$ is defined analogously to Equation (12.19)

$$d\boldsymbol{\varepsilon} = \tfrac{1}{2}[(\nabla d\mathbf{u}) + (\nabla d\mathbf{u})^T] \qquad (12.21)$$

and the 'Jaumann change' $d^J\boldsymbol{\sigma}$ is related to the change in the rotation-neutralized stress tensor by

$$d^J\boldsymbol{\sigma} = \mathbf{R}\cdot d\bar{\boldsymbol{\sigma}}\cdot\mathbf{R}^T \qquad (12.22)$$

In Equation (12.20), the linearized form of the right-hand side is presented in symbolic form. Correct derivation of this linearized form is important in order to obtain a good solution procedure; however, this aspect will not be discussed in this paper. From the integrated constitutive equation for the rotation-neutralized stress tensor given by Equation (12.16), a linearized relation of the type

$$d\bar{\boldsymbol{\sigma}} = \bar{\mathbf{M}}:d\bar{\mathbf{C}} \qquad (12.23)$$

can be derived. The derivation of the moduli $\bar{\mathbf{M}}$ is discussed in the next section. Here we concentrate on the calculation of $d\bar{\mathbf{C}}$.

The expression for $\bar{\mathbf{C}}$ itself was derived in Section 12.2, and is given by Equation (12.15). Unfortunately, Equation (12.15) cannot be linearized directly, a series expansion must be used to obtain a tractable form. Hence we write

$$\mathbf{U} = \mathbf{I} + \mathbf{e} \qquad (12.24)$$

where $\mathbf{e}$ is the engineering strain tensor. Equation (12.15) may then be written in series form:

$$\bar{\mathbf{C}} = \mathbf{e} - \tfrac{1}{2}\mathbf{e}\cdot\mathbf{e} + \tfrac{1}{3}\mathbf{e}\cdot\mathbf{e}\cdot\mathbf{e} - \ldots \qquad (12.25)$$

This equation is readily linearized, which yields

$$d\bar{\mathbf{C}} = d\mathbf{e} - \tfrac{1}{2}(\mathbf{e}\cdot d\mathbf{e} + d\mathbf{e}\cdot\mathbf{e}) + \tfrac{1}{3}(\mathbf{e}\cdot\mathbf{e}\cdot d\mathbf{e} + \mathbf{e}\cdot d\mathbf{e}\cdot\mathbf{e} + d\mathbf{e}\cdot\mathbf{e}\cdot\mathbf{e}) - \ldots \qquad (12.26)$$

In order to relate $d\bar{\mathbf{C}}$ to change in displacement $d\mathbf{u}$, consider Equation (12.21) for $d\boldsymbol{\varepsilon}$. This relation may also be written as

$$d\boldsymbol{\varepsilon} = \tfrac{1}{2}[\mathbf{F}^{-T}\cdot d\mathbf{F}^T + d\mathbf{F}\cdot\mathbf{F}^{-1}] \qquad (12.27)$$

If this equation is neutralized for rotation, it transforms into

$$d\bar{\boldsymbol{\varepsilon}} = \mathbf{R}^T\cdot d\boldsymbol{\varepsilon}\cdot\mathbf{R} = \tfrac{1}{2}[\mathbf{U}^{-1}\cdot d\mathbf{U} + d\mathbf{U}\cdot\mathbf{U}^{-1}] \qquad (12.28)$$

where use is made of Equation (12.14) and of the orthogonality of $\mathbf{R}$. Substitution of Equations (12.24) in (12.28) and use of a series expansion for $\mathbf{U}^{-1}$ gives

$$\mathbf{U}^{-1} = \mathbf{I} - \mathbf{e} + \mathbf{e}\cdot\mathbf{e} - \mathbf{e}\cdot\mathbf{e}\cdot\mathbf{e} + \ldots \qquad (12.29)$$

which then yields an expression for $d\bar{\boldsymbol{\varepsilon}}$ in terms of $\mathbf{e}$ and $d\mathbf{e}$

$$d\bar{\boldsymbol{\varepsilon}} = d\mathbf{e} - \tfrac{1}{2}(\mathbf{e}\cdot d\mathbf{e} + d\mathbf{e}\cdot\mathbf{e}) + \tfrac{1}{2}(\mathbf{e}\cdot\mathbf{e}\cdot d\mathbf{e} + d\mathbf{e}\cdot\mathbf{e}\cdot\mathbf{e}) - \ldots \qquad (12.30)$$

For a normal plasticity analysis, the strain increment will usually be considerably smaller than unity, hence higher-order terms in Equations (12.26) and (12.30) will decrease rapidly in magnitude. Hence, the following relation is valid with good approximation

$$d\bar{\mathbf{C}} \simeq d\bar{\boldsymbol{\varepsilon}} = \mathbf{R}^T\cdot d\boldsymbol{\varepsilon}\cdot\mathbf{R} \qquad (12.31)$$

Combination of Equations (12.20), (12.22), (12.23) and (12.31) then furnishes the final variational equation:

$$\int_V \{d\boldsymbol{\varepsilon}:\mathbf{M}:\delta\boldsymbol{\varepsilon} - 2(d\boldsymbol{\varepsilon}\cdot\boldsymbol{\sigma}):\delta\boldsymbol{\varepsilon} + \operatorname{tr}(d\boldsymbol{\varepsilon})\boldsymbol{\sigma}:\delta\boldsymbol{\varepsilon} + \boldsymbol{\sigma}:[(\nabla d\mathbf{u})\cdot(\nabla\delta\mathbf{u})^T]\}dV$$

$$= d\int_V \mathbf{q}\cdot\delta\mathbf{u}\,dV + d\int_S \mathbf{p}\cdot\delta\mathbf{u}\,dS \qquad (12.32)$$

with

$$\mathbf{M} = \mathbf{R}\cdot[\mathbf{R}\cdot\bar{\mathbf{M}}\cdot\mathbf{R}^T]\cdot\mathbf{R}^T \qquad (12.33)$$

Note that the moduli $\mathbf{M}$ will not usually not calculated from the rotation-neutralized moduli $\bar{\mathbf{M}}$ with Equation (12.33), but can be obtained directly from the (unrotated) stress tensor $\boldsymbol{\sigma}$, and eventually other tensor quantities $\boldsymbol{\alpha}_i$.

In a finite element scheme the term $\operatorname{tr}(d\boldsymbol{\varepsilon})\boldsymbol{\sigma}:\delta\boldsymbol{\varepsilon}$ will lead to a nonsymmetrical stiffness matrix. This term stems from the change of volume in successive iteration and is usually neglected. Equation (12.32) is in complete agreement with the analogous equation following from the variational rate principle due to Hill[8] and used by McMeeking and Rice in an earlier paper[3] on this subject. However, there is one essential difference. In Equation (12.32) the so-called 'linearization moduli' $\mathbf{M}$ are used, whereas McMeeking and Rice used the standard tangent moduli $\mathbf{L}$ as given in Equation (12.1). As will be seen in the next section, the difference between the two is substantial, particularly if the strain increments are large compared with the elastic strains.

12.4 THE INTEGRATED CONSTITUTIVE EQUATIONS

The last steps to complete the formulation are the calculation of the stress tensor $\boldsymbol{\sigma}_e$ from Equations (12.16) and (12.17) and the determination of the moduli $\mathbf{M}$. The integration procedure for Equation (12.16) will not be discussed here, any suitable procedure may be used. Krieg and Krieg[9] made a study of various simple procedures. For von Mises plasticity without hardening they found that the radial return method is both accurate and effective.

Here we concentrate on the determination of the moduli $\mathbf{M}$. Since $\bar{\mathbf{D}}$ is assumed to be constant and equal to $(1/\Delta t)\bar{\mathbf{C}}$ it follows from Equation (12.11) that

$$\bar{\mathbf{M}} = \frac{1}{\Delta t}\int_{t_0}^{t_e} \bar{\mathbf{L}}\,\mathrm{d}t + \left[\frac{1}{\Delta t}\int_{t_0}^{t_e} (\partial\mathbf{L}/\partial\bar{\mathbf{C}})\,\mathrm{d}t\right]:\bar{\mathbf{C}} \tag{12.34}$$

The second term is not obtained if one just uses the constitutive rate equations directly. Particularly if the incremental strains are large, this term is very important, as will become apparent later.

In general it is impossible to derive an analytical expression for $\bar{\mathbf{M}}$. If a simple integration procedure is chosen, however, an approximation for $\bar{\mathbf{M}}$ may be obtained in an analytical way and the importance of the second term in Equation (12.34) can be evaluated. To illustrate this, we consider von Mises plasticity with hardening. Then the moduli $\bar{\mathbf{L}}$ in Equation (12.11) are given by

$$\bar{\mathbf{L}} = k\mathbf{II} + 2G\left[\mathbf{I} - \tfrac{1}{3}\mathbf{II} - \tfrac{3}{2}\mu\frac{\bar{\boldsymbol{\sigma}}^d\bar{\boldsymbol{\sigma}}^d}{\sigma_y^2}\right]; \qquad \mu = \left(1 + \frac{h}{3G}\right)^{-1} \tag{12.35}$$

where G is the shear modulus, k is the bulk modulus, σ_y is the current yield stress, h is the plastic hardening coefficient and $\bar{\boldsymbol{\sigma}}^d = \bar{\boldsymbol{\sigma}} - \frac{1}{3}\mathrm{tr}(\bar{\boldsymbol{\sigma}})\mathbf{I}$ is the deviatoric part of $\bar{\boldsymbol{\sigma}}$. Both h and σ_y can depend on the equivalent plastic strain $\bar{\varepsilon}^p$

$$\dot{\bar{\varepsilon}}^p = \mu\frac{\bar{\boldsymbol{\sigma}}^{a}:\bar{\mathbf{D}}}{\sigma_y}; \qquad h = \frac{\mathrm{d}\sigma_y}{\mathrm{d}\bar{\varepsilon}^p} \tag{12.36}$$

As in Section 17.2 we denote a quantity ϕ at the beginning and end of the increment by ϕ_0 and ϕ_e. From Equation (12.16) it follows that

$$\bar{\boldsymbol{\sigma}}_e = \bar{\boldsymbol{\sigma}}_0 + k\,\mathrm{tr}(\bar{\mathbf{C}})\mathbf{I} + 2G\bar{\mathbf{C}}^d - 3G\int_{t_0}^{t_e}\frac{\dot{\bar{\varepsilon}}^p}{\sigma_y}\bar{\boldsymbol{\sigma}}^d\,\mathrm{d}t \tag{12.37}$$

where $\bar{\mathbf{C}}^d$ is the deviatoric part of $\bar{\mathbf{C}}$. To evaluate the remaining integral, a very simple integration procedure, given by

$$\int_{t_0}^{t_e}\phi(t)\,\mathrm{d}t = (t_e - t_0)[\beta\phi_0 + (1-\beta)\phi_e] \qquad 0 \leqslant \beta < 1 \tag{12.38}$$

is chosen. Then it is readily established that

$$[1 + (1-\beta)\gamma_e]\bar{\boldsymbol{\sigma}}_e^d = \bar{\boldsymbol{\sigma}}_n; \qquad \bar{\boldsymbol{\sigma}}_n = (1 - \beta\gamma_0)\bar{\boldsymbol{\sigma}}_0^d + 2G\bar{\mathbf{C}}^d \tag{12.39}$$

where the scalar quantity $\gamma(t)$ is defined by:

$$\gamma = 3G\frac{\dot{\bar{\varepsilon}}^p}{\sigma_y}\Delta t = 3G\mu\frac{\bar{\boldsymbol{\sigma}}^d:\bar{\mathbf{C}}^d}{\sigma_y^e} \tag{12.40}$$

As soon as $\bar{\mathbf{C}}$ is known, $\gamma_0 = (t_0)$ and the stress tensor $\bar{\boldsymbol{\sigma}}_n$, introduced in Equation

(12.39), can be determined. In the radial return method, the unknown factor $[1 + (1-\beta)\gamma_e]$ in Equation (12.39) follows from the requirement that $\bar{\boldsymbol{\sigma}}_e$ satisfies the yield condition

$$\tfrac{3}{2}\bar{\boldsymbol{\sigma}}_e^d:\bar{\boldsymbol{\sigma}}_e^d = \sigma_{ye}^2$$

at the end of the increment. This results in

$$\bar{\boldsymbol{\sigma}}_e^d = \alpha_a\bar{\boldsymbol{\sigma}}_n; \qquad \alpha_e = \frac{\sigma_{ye}}{\bar{\sigma}_n}; \qquad \bar{\sigma}_n = \sqrt{\tfrac{3}{2}\bar{\boldsymbol{\sigma}}_n:\bar{\boldsymbol{\sigma}}_n} \tag{12.41}$$

Using $\mathrm{tr}(\bar{\boldsymbol{\sigma}}_e) = \mathrm{tr}(\bar{\boldsymbol{\sigma}}_0) + 3k\,\mathrm{tr}(\bar{\mathbf{C}})$, we finally arrive at

$$\bar{\boldsymbol{\sigma}}_e = [\tfrac{1}{3}\mathrm{tr}(\bar{\boldsymbol{\sigma}}_0) + k\,\mathrm{tr}(\bar{\mathbf{C}})]\mathbf{I} + \alpha_e\bar{\boldsymbol{\sigma}}_n \tag{12.42}$$

where $\bar{\boldsymbol{\sigma}}_n$ is defined in Equation (12.39).

The moduli $\bar{\mathbf{M}}$ relate the change $\mathrm{d}\bar{\boldsymbol{\sigma}}_e$ to the change $\mathrm{d}\bar{\mathbf{C}}$ in successive iteration steps. Using Equations (12.41) and (12.42), it is readily seen that

$$\mathrm{d}\bar{\boldsymbol{\sigma}}_e = k\mathbf{II}:d\bar{\mathbf{C}} + \alpha_e\left[\left(\frac{\mathrm{d}\sigma_{ye}}{\sigma_{ye}} - \frac{\mathrm{d}\bar{\sigma}_n}{\bar{\sigma}_n}\right)\bar{\boldsymbol{\sigma}}_n + \mathrm{d}\bar{\boldsymbol{\sigma}}_n\right] \tag{12.43}$$

Due to the definitions of the strain hardening coefficient h, Equation (12.36) of the stress tensors $\bar{\boldsymbol{\sigma}}_n$ and of the equivalent stress, $\bar{\sigma}_n$, Equation (12.41), it is easy to show that

$$\mathrm{d}\bar{\boldsymbol{\sigma}}_e = k\mathbf{II}:\mathrm{d}\bar{\mathbf{C}} + 2G\alpha_e\left[\mathbf{I} - \frac{3}{2}\frac{\bar{\boldsymbol{\sigma}}_n\bar{\boldsymbol{\sigma}}_n}{\bar{\sigma}_n^2}\right]:\mathrm{d}\bar{\mathbf{C}}^d + \alpha_e\frac{h\,\mathrm{d}^{-p}}{\sigma_{ye}^2}\bar{\boldsymbol{\sigma}}_n \tag{12.44}$$

The term $\mathrm{d}\bar{\varepsilon}^p$ in this expression is unknown and must be related to $\mathrm{d}\bar{\mathbf{C}}$. From the definition Equation (12.36) of $\dot{\bar{\varepsilon}}^p$ and from

$$\bar{\mathbf{D}} = \frac{1}{\Delta t}\bar{\mathbf{C}}$$

it is seen that a reasonable approximation for $\mathrm{d}\bar{\varepsilon}^p$ will be given by

$$\mathrm{d}\bar{\varepsilon}^p = \mu_e\frac{\bar{\boldsymbol{\sigma}}_e^d:\mathrm{d}\bar{\mathbf{C}}}{\sigma_{ye}} = \mu_e\frac{\bar{\boldsymbol{\sigma}}_n:\mathrm{d}\bar{\mathbf{C}}}{\bar{\sigma}_n} \tag{12.45}$$

Substitution in Equation (12.44) and introduction of the so-called effective shear modulus G^* and the effective strain hardening coefficient h^*,

$$G^* = \alpha_e G = \frac{\sigma_{ye}}{\bar{\sigma}_n}G; \qquad \mu^* = 1 - \frac{1-\mu_e}{\alpha_e} = \left(1 + \frac{h^*}{3G}\right)^{-1} \tag{12.46}$$

finally yields the desired relation for $\bar{\mathbf{M}}$

$$\mathrm{d}\bar{\boldsymbol{\sigma}}_e = \bar{\mathbf{M}}:\mathrm{d}\bar{\mathbf{C}}; \qquad \bar{\mathbf{M}} = k\mathbf{II} + 2G^*\left[(\mathbf{I} - \tfrac{1}{3}\mathbf{II}) - \tfrac{3}{2}\mu^*\frac{\bar{\boldsymbol{\sigma}}_n\bar{\boldsymbol{\sigma}}_n}{\bar{\sigma}_n^2}\right] \tag{12.47}$$

Hence the expression for $\bar{\mathbf{M}}$ has exactly the same form as the relation for the moduli $\bar{\mathbf{L}}$ in the standard rate Equation (12.10) for plasticity. However, the shear modulus and the hardening coefficient are modified and the stress $\bar{\sigma}_0^d$ is replaced by $\bar{\sigma}_n = (1-\beta\gamma_0)\bar{\sigma}_0^d + 2G\bar{\mathbf{C}}^d$. If the so-called elastic stress increment $2G\bar{\mathbf{C}}^d$ is large compared with $\bar{\sigma}_0^d$, the effective shear modulus $G^* = \alpha_e G$ is reduced considerably with respect to the shear modulus G since in that case α_e is much smaller than 1. Thus, use of the moduli $\bar{\mathbf{L}}$ instead of $\bar{\mathbf{M}}$ can lead to a very slow convergence.

Finally, it should be noted that the unrotated moduli $\mathbf{M}$ which are needed in the variational statement Equation (12.32), can be readily obtained in explicit form. Substitution of Equation (12.47) in (12.33) yields

$$\mathbf{M} = k\mathbf{II} + 2G^*\left[(\mathbf{I} - \tfrac{1}{3}\mathbf{II}) - \tfrac{3}{2}\mu^* \frac{\boldsymbol{\sigma}_n\boldsymbol{\sigma}_n}{\sigma_n^2}\right] \tag{12.48}$$

with

$$\boldsymbol{\sigma}_n/\sigma_n = \boldsymbol{\sigma}_e^d/\sigma_{ye}; \qquad \boldsymbol{\sigma}_e^d = \boldsymbol{\sigma}_e - \tfrac{1}{3}\mathrm{tr}(\boldsymbol{\sigma}_e)\mathbf{I} \tag{12.49}$$

Hence, a simple expression is available to evaluate the moduli directly from the last obtained solution for $\boldsymbol{\sigma}_e$.

12.5 IMPLEMENTATION IN A FINITE ELEMENT PROGRAM

From Section 12.3, dealing with the variational formulation, it is quite clear that in the procedure presented here it is attempted to satisfy equilibrium in the current state of the body. Moreover during iteration, the nodal imbalance is formulated with respect to the state obtained as a result of the previous iteration. Hence, upon calculation of the latest estimate for the displacement increment, the geometry of the elements will be updated corresponding to this latest estimate.

The first step that must be taken after a new calculation of the displacement increment is the calculation of the (constant, rotation-neutralized) deformation rate tensor $\bar{\mathbf{C}}/\Delta t$ via Equation (12.15). The most direct way would be to calculate $\bar{\mathbf{C}}/\Delta t$ from $\mathbf{U}$, which is in turn obtained through polar decomposition of $\mathbf{F}$. This approach however, is not so suitable for numerical implementation, in particular if at some stage in the analysis only small, elastic strain increments occur. In that case $\mathbf{U}$ will differ very little from the identity tensor $\mathbf{I}$, and the eigenvalues λ_i of $\mathbf{U}$ may have large errors relative to the actual strain increment. Hence it is better to calculate principal strain increments directly from the displacement increment. Because the geometry was updated, gradients of the displacement increment can only be taken with respect to the current state. These 'gradients in the current state' can be used to calculate the Almansi strain tensor for the increment:

$$\boldsymbol{\varepsilon}^{\mathrm{A}} = \tfrac{1}{2}[(\nabla\Delta\mathbf{u}) + (\nabla\Delta\mathbf{u})^{\mathrm{T}} - (\nabla\Delta\mathbf{u})\cdot(\nabla\Delta\mathbf{u})^{\mathrm{T}}] \tag{12.50}$$

with $\Delta\mathbf{u}$ the displacement increment. In terms of principal values, this can be written as

$$\boldsymbol{\varepsilon}^{\mathrm{A}} = \sum_{i=1}^{3} \varepsilon_i^{\mathrm{A}} \mathbf{n}_i\mathbf{n}_i$$

where $\mathbf{n}_i$ are the principal directions in the updated state. From the principal values of the Almansi tensor, the principal values of $\mathbf{U}$ can be calculated via the relation

$$\lambda_i = (1 - 2\varepsilon_i^{\mathrm{A}})^{-1/2} \tag{12.51}$$

which is readily derived from Equation (12.50). The principal values of $\bar{\mathbf{C}}$ then follow from Equation (12.15), which combined with Equation (12.51) yields

$$\bar{\mathbf{C}}_i = \ln(\lambda_i) = -\tfrac{1}{2}\ln(1 - 2\varepsilon_i^{\mathrm{A}}) \tag{12.52}$$

As in the calculation of $\ln(\lambda_i)$ from $\mathbf{F}$, direct evaluation of Equation (12.52) yields inaccurate results for small $\varepsilon_i^{\mathrm{A}}$. Hence, for $\varepsilon_i^{\mathrm{A}} < 0.01$, the following series expansion is used:

$$\bar{\mathbf{C}}_i = ((\varepsilon_i^{\mathrm{A}}) + (\varepsilon_i^{\mathrm{A}})^2 + \tfrac{4}{3}(\varepsilon_i^{\mathrm{A}})^3 + 2(\varepsilon_i^{\mathrm{A}})^4 + \cdots) \tag{12.53}$$

With Equations (12.52) and (12.53), the deformation rate can be calculated accurately for any value of the displacement.

It remains to calculate the eigenvectors $\mathbf{N}_i$ with respect to the state at the beginning at the increment. Therefore, one must first calculate the rotation tensor $\mathbf{R}$ from the polar decomposition of $\mathbf{F}$, Equation (12.14). The eigenvector $\mathbf{N}_i$ then follows by rotating the eigenvectors $\mathbf{n}_i$ with respect to the state at the end of the increment:

$$\mathbf{N}_i = \mathbf{R}^{\mathrm{T}}\cdot\mathbf{n}_i \tag{12.54}$$

The last calculations can be carried out directly without the danger that large relative errors will occur.

The formulation of the stiffness matrix is again carried out in the state updated according to the latest estimate for the displacement increment. Once the updating is done, the implementation follows the equations in Section 12.3 precisely.

12.6 APPLICATIONS

The formulation presented in this paper was implemented in a development version of the MARC finite element program,[10] and a number of calculations were carried out. Some of the calculations were carried out with different increment size, in order to test whether the attempted independence of increment size was obtained.

Prior to the solution of practical problems, a number of one-element tests were carried out to check the correctness of the implementation. In uniaxial loading tests, results were obtained with any step size, and perfect agreement was reached with analytical solutions. For biaxial tests, complete independence of increment size was also obtained. However, it was observed that after a change in loading direction the increment size had to be limited somewhat (to increment sizes in the order of 10% strain) in order for the Newton–Raphson method to converge. The same holds true for simple shear tests. Here, a shear strain increment size of 10% yields rapid convergence. In simple shear the results are not completely exact. However, the agreement with analytical results is still so close that in a plot of force versus displacement the numerical results are indistinguishable from the analytical results.

The next problem concerns the axisymmetric upsetting of a disk. The disk shown in Figure 12.1 has a height of 12 units, a radius of 10, and is bonded to a rigid punch. The yield stress was arbitrarily chosen as 1, the modulus was chosen at 1000, and Poisson's ratio was chosen equal to 0.3. The total stress–strain curve is also shown in Figure 12.1. A mesh of 60 quadrilateral axisymmetric constant dilatation elements was used in this analysis. MARC gap elements were used to ensure that the free surface on the outside radius could not penetrate the punch. The analysis was first carried out with prescribed displacement increments of the punch of 1% of the original height. A total height reduction of 44% was obtained, after which the analysis terminated because one of the elements turned inside-out. The load–deflection curve is shown in Figure 12.2 and the final distorted mesh is shown in Figure 12.3. The jump in the load–deflection curve occurs when the first node on the outside boundary comes in contact with the punch, and the contact area suddenly increases. With a finer mesh, or a more sophisticated contact modelling procedure, this jump could be decreased considerably. On the average, about four Newton–Raphson iterations were needed to get a convergent solution in each increment. The analysis was repeated with a step size five times smaller. Now, about three Newton–Raphson iterations were needed in each increment. The results were virtually indistinguishable: the maximum difference in load was about 0.5%. The analysis was re-run with the standard version of MARC, which uses a linearized strain increment calculation and a mid-increment plasticity

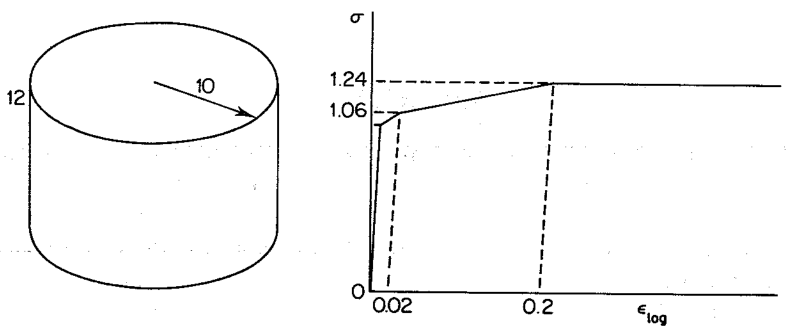

Figure 12.1 Force versus displacement: new algorithm

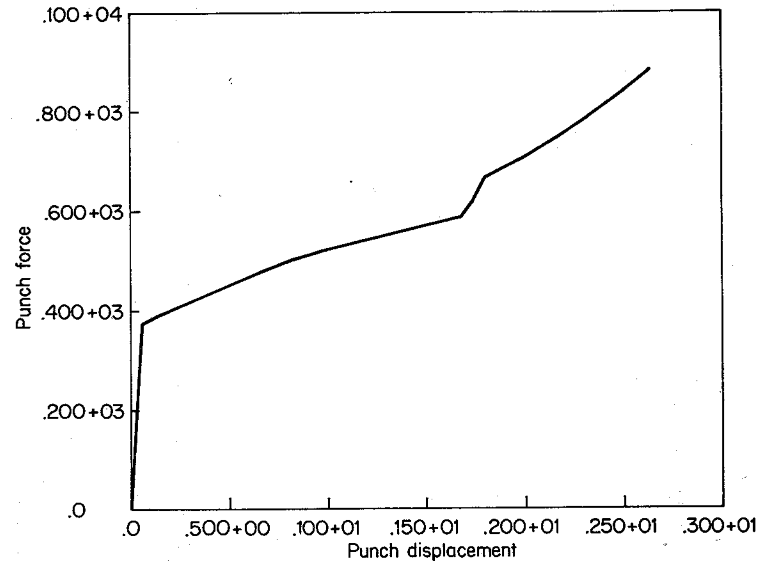

Figure 12.2 Force versus displacement: new algorithm

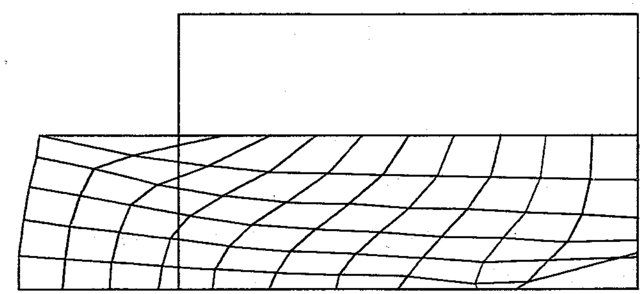

Figure 12.3 Upsetting: deformed mesh after 44% height reduction

algorithm.[5] For small load steps, this yields virtually the same results as were obtained in the analyses with the current procedure (differences of up to 1.5%). However, if the step is chosen equal to 1% height reduction, large oscillations in total load start to occur after the node of the free surface gets in contact with the punch, as is shown in Figure 12.4. The procedure used in the standard version of MARC has obvious difficulties with convergence due to the sudden change in loading direction. Although an increased number of iterations might improve the results somewhat, drastic improvement may not be expected.

The final problem is the extrusion of a cylindrical bar through a smooth die with

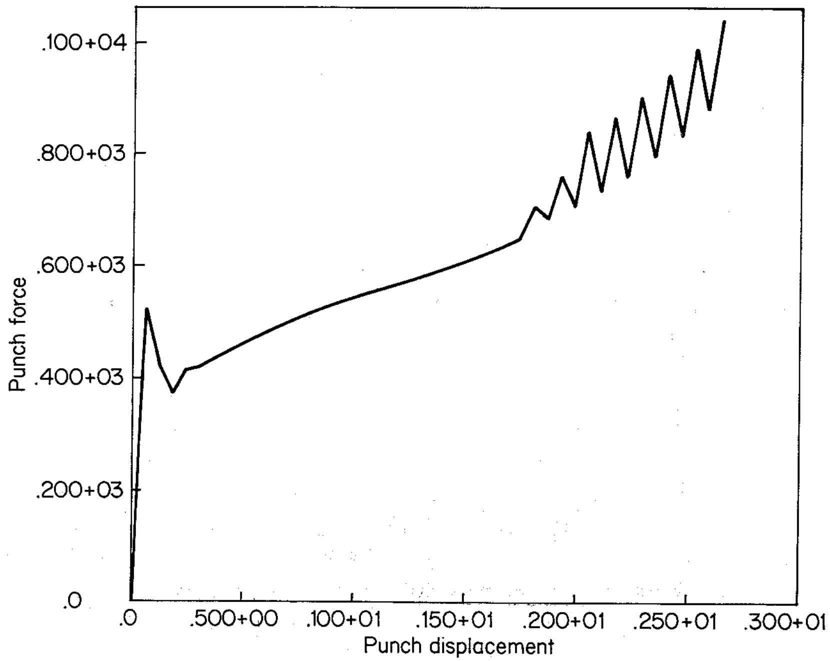

Figure 12.4 Force versus displacement: old algorithm

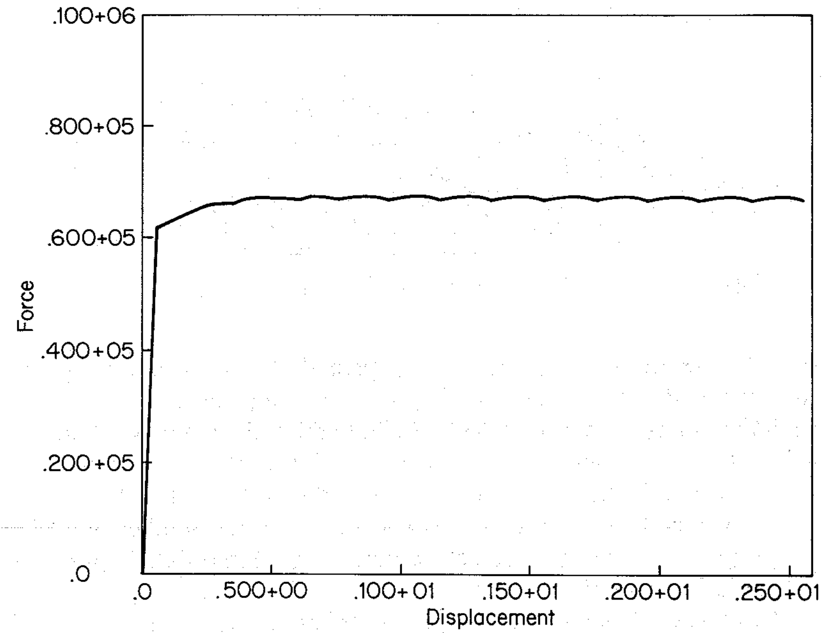

Figure 12.5 Extrusion force versus piston displacement

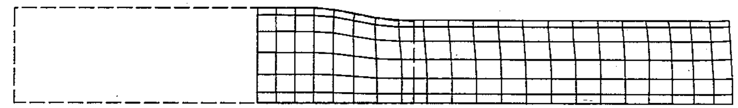

Figure 12.6 Deformed mesh at end of extrusion

a reduction of cross-sectional area of 25%. Problems of this type were analysed by various investigators.[11,12] In this problem, a prescribed piston displacement of 1/20 of the initial radius of 1.0 was used. The material had slight work-hardening levelling-off after ~5% plastic strain. The load–displacement curve and the deformed mesh, after 50 increments with a total displacement of 2.5 times the initial radius, are shown in Figure 12.5 and Figure 12.6, respectively. Note that due to the fact that a discrete model is used, a non-smooth load–displacement curve is obtained. The oscillation in the load, however, is only about 1% of the total load. This problem was also analyzed by Wertheimer[13] with the standard version of the MARC program with a displacement increment five times smaller. With this version, the load initially increases to about 9% over the steady-state load. The steady-state load obtained by Wertheimer agreed to within 1% with the load obtained with the current procedure.

Use of larger load steps in both the upsetting and the extrusion problem produce good results for a few increments which, however, then failed to converge for subsequent increments. Hence it is believed that with an improved iteration procedure the load increments could be further increased without a significant loss of accuracy.

APPENDIX 12A. EXPONENTIAL AND LOGARITHMIC FUNCTIONS OF SYMMETRIC TENSORS

In Section 12.2, Equations (12.13) and (12.15) deal with logarithmic and exponential tensor functions. These functions were introduced to obtain a solution to the tensor differential Equation (12.12). The exponential and logarithmic tensor functions are evaluated by using a representation in principal directions and principal values (spectral representation). Consider for instance the symmetric tensor $\bar{\mathbf{C}}$. In spectral representation, this tensor may be written as:

$$\bar{\mathbf{C}} = \sum_{i=1}^{3} \bar{C}_i \mathbf{N}_i \mathbf{N}_i \qquad (12A.1)$$

where $\bar{C}_i$ and $\mathbf{N}_i$ are principal values and directions, respectively. The exponential tensor function, Equation (12.13), which yields the tensor $\bar{\mathbf{F}}$, is then evaluated as

$$\bar{\mathbf{F}} = \sum_{i=1}^{3} \bar{F}_i \mathbf{N}_i \mathbf{N}_i = \sum_{i=1}^{3} \exp\left(\frac{t - t_0}{\Delta} \bar{C}\right) \mathbf{N}_i \mathbf{N}_i \qquad (12A.2)$$

Differentiation of $\bar{\mathbf{F}}$ with respect to time yields

$$\dot{\bar{\mathbf{F}}}=\sum_{i=1}^{3}\frac{1}{\Delta t}\bar{C}_i\bar{F}_i\mathbf{N}_i\mathbf{N}_i \tag{12A.3}$$

and since

$$\bar{\mathbf{F}}^{-1}=\sum_{i=1}^{3}\bar{F}_i^{-1}\mathbf{N}_i\mathbf{N}_i \tag{12A.4}$$

it follows that

$$\dot{\bar{\mathbf{F}}}\cdot\bar{\mathbf{F}}^{-1}=\sum_{i=1}^{3}\frac{1}{\Delta t}\bar{C}\mathbf{N}_i\mathbf{N}_i=\frac{1}{\Delta t}\bar{C} \tag{12A.5}$$

which proves that the tensor function $\bar{\mathbf{F}}$ defined by Equation (12.13) satisfies the tensor differential Equation (12.12).

Logarithmic tensor functions are treated similarly. Hence Equation (12.15) may be written in the form

$$\bar{\mathbf{C}}=\sum_{i=1}^{3}\bar{C}_i\mathbf{N}_i\mathbf{N}_i=\sum_{i=1}^{3}\ln(\lambda_i)\mathbf{N}_i\mathbf{N}_i=\ln(\mathbf{U}) \tag{12A.6}$$

where λ_i are the eigenvalues of $\mathbf{U}$.

APPENDIX 12B. APPROXIMATE AND ACTUAL DEFORMATION RATE IN SIMPLE SHEAR

Consider the velocity and displacement fields in simple shear. With reference to Figure 12.7, it is readily established that

$$v_1=\dot{\gamma}y, \qquad v_2=0, \qquad u_1=\dot{\gamma}ty, \qquad u_2=0 \tag{12B.1}$$

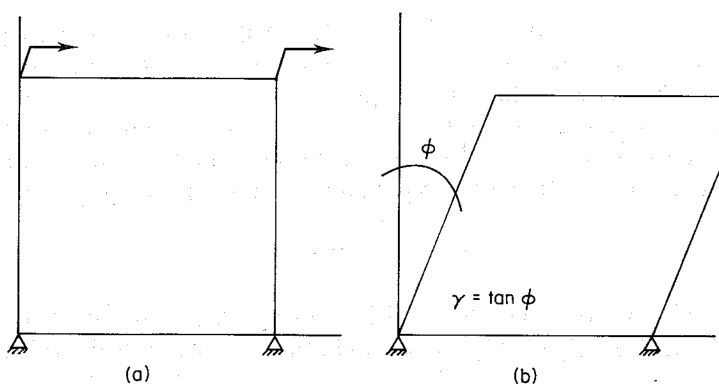

Figure 12.7 Simple shear test.

For this field, one can readily calculate the actual and the approximate rotation neutralized deformation rate.

(a) Actual rotation neutralized deformation rate

The standard deformation rate tensor is (in matrix form)

$$\mathbf{D}=\tfrac{1}{2}[(\nabla\mathbf{v})^{\mathrm{T}}+(\nabla\mathbf{v})]=\begin{bmatrix}0 & \tfrac{1}{2}\dot{\gamma}\\ \tfrac{1}{2}\dot{\gamma} & 0\end{bmatrix} \tag{12B.2}$$

The standard spin tensor is

$$\mathbf{\Omega}=\tfrac{1}{2}[(\nabla\mathbf{v})^{\mathrm{T}}-(\nabla\mathbf{v})]=\begin{bmatrix}0 & \tfrac{1}{2}\dot{\gamma}\\ -\tfrac{1}{2}\dot{\gamma} & 0\end{bmatrix} \tag{12B.3}$$

From Equation (12.6) may be derived the set of coupled first-order differential equations:

$$\dot{\rho}_{11}=\tfrac{1}{2}\dot{\gamma}\rho_{12}, \qquad \dot{\rho}_{12}=\tfrac{1}{2}\dot{\gamma}\rho_{22}, \qquad \dot{\rho}_{21}=\tfrac{1}{2}\dot{\gamma}\rho_{11}, \qquad \dot{\rho}_{22}=\tfrac{1}{2}\dot{\gamma}\rho_{12} \tag{12B.4}$$

With the appropriate initial conditions, the solution for the material rotation tensor is readily obtained as

$$\mathbf{f}(\gamma)=\begin{bmatrix}\cos\tfrac{1}{2}\gamma & \sin\tfrac{1}{2}\gamma\\ -\sin\tfrac{1}{2}\gamma & \cos\tfrac{1}{2}\gamma\end{bmatrix} \tag{12B.5}$$

The actual rotation-neutralized deformation tensor is found by substitution of Equation (12B.2) and (12B.5) in (12.7c), which yields after some arithmetic,

$$\bar{\mathbf{D}}(\gamma)=\tfrac{1}{2}\dot{\gamma}\begin{bmatrix}-\sin\gamma & \cos\gamma\\ \cos\gamma & \sin\gamma\end{bmatrix} \tag{12B.6}$$

It is clear from the above that the rotation-neutralized deformation rate is a function of the shear angle γ. The equivalent strain rate, however, is constant:

$$|\bar{\mathbf{D}}|=\sqrt{\tfrac{2}{3}\bar{\mathbf{D}}:\bar{\mathbf{D}}}=\frac{1}{\sqrt{3}}\dot{\gamma} \tag{12B.7}$$

(b) Approximate rotation-neutralized deformation rate

The first step to obtain the approximate rate is to calculate the deformation tensor

$$\mathbf{F}=\mathbf{I}+(\nabla\mathbf{u})^{\mathrm{T}}=\begin{bmatrix}1 & \gamma\\ 0 & 1\end{bmatrix} \tag{12B.8}$$

The next step is to make the polar decomposition of $\mathbf{F}$ according to Equation

(12.14). This may be written as the following matrix equation:

$$\mathbf{F}=\mathbf{R}\cdot\mathbf{U}=\begin{bmatrix}\cos\phi & \sin\phi\\ -\sin\phi & \cos\phi\end{bmatrix}\begin{bmatrix}U_{11} & U_{12}\\ U_{12} & U_{22}\end{bmatrix}=\begin{bmatrix}1 & \gamma\\ 0 & 1\end{bmatrix} \qquad (12B.9)$$

where both the angle ϕ and the components of $\mathbf{U}$ must be determined. After the necessary calculations,

$$\mathbf{U}=\begin{bmatrix}\cos\phi & \sin\phi\\ \sin\phi & 1+\sin\phi\tan\phi\end{bmatrix} \qquad (12B.10)$$

with

$$\tan\phi=\tfrac{1}{2}\gamma \qquad (12B.11)$$

Subsequently the principal values and principal directions of the symmetric tensor $\mathbf{U}$ must be calculated. After a fairly lengthy but straightforward calculation,

$$\begin{aligned}&\lambda_2=(1-\sin\phi)/\cos\phi, \qquad \lambda_2=(1-\sin\phi)/\cos\phi\\ &\mathbf{N}_1=(2-2\sin\phi)^{-1/2}\begin{bmatrix}1-\sin\phi\\ \cos\phi\end{bmatrix}\\ &\mathbf{N}_2=(2-2\sin\phi)^{-1/2}\begin{bmatrix}\cos\phi\\ \sin\phi-1\end{bmatrix}\end{aligned} \qquad (12B.12)$$

Substitution in Equation (12A.6) then yields the approximate deformation rate

$$\begin{aligned}\frac{1}{\Delta t}\bar{\mathbf{C}}&=\frac{1}{\Delta t}\sum_i \ln\lambda_i\mathbf{N}_i\mathbf{N}_i\\ &=\frac{\dot{\gamma}}{2}\cot\phi\ln\left(\frac{1+\sin\phi}{\cos\phi}\right)\begin{bmatrix}-\sin\phi & \cos\phi\\ \cos\phi & \sin\phi\end{bmatrix}\end{aligned} \qquad (12B.13)$$

By definition, the approximate tensor is constant, the equivalent approximate strain rate is

$$\left|\frac{1}{\Delta t}\bar{\mathbf{C}}\right|=\sqrt{\tfrac{2}{3}\bar{\mathbf{D}}^0:\bar{\mathbf{D}}^0}=\frac{1}{\sqrt{3}}\dot{\gamma}\cot\phi\ln\left(\frac{1+\sin\phi}{\cos\phi}\right) \qquad (12B.14)$$

From the above, it is clear that several differences between the exact and approximate rotation-neutralized deformation rates exist for simple shear. For simple shear, the exact rate varies in direction; the approximate rate has a constant direction, which is approximately equal to the average direction of the exact deformation rate. For isotropically hardening materials, this difference in direction is not very significant. However, for such materials the difference in equivalent strain rate is of importance. This difference readily follows from

Equations (12B.7) and (12B.14),

$$\left|\frac{1}{\Delta t}\bar{\mathbf{C}}\right|=\cot\phi\ln\left(\frac{1+\sin\phi}{\cos\phi}\right)|\bar{\mathbf{D}}|=\alpha(\gamma)|\bar{\mathbf{D}}| \qquad (12B.15)$$

As shown in Table 12.1, the factor $\alpha(\gamma)$ is approximately equal to 1 for $0<\gamma<1$.

APPENDIX 12C. DERIVATION OF THE LINEARIZED VARIATIONAL FORM

In order to obtain a linearized variational form, one first has to rewrite the virtual-work equation so that it refers to a fixed reference state. This means that the virtual-work equation must be written so that all integrations are carried out and gradients are taken in this fixed state. The natural choice for this is the state at the beginning of the increment. Hence Equation (12.18) is written as

$$\int_{V_0}[(\mathbf{F}^{-1}\cdot\boldsymbol{\sigma}):\delta\mathbf{F}]J\,dV=\int_V \mathbf{q}\cdot\delta\mathbf{u}\,dV+\int_S \mathbf{p}\cdot\delta\mathbf{u}\,dS \qquad (12C.1)$$

where $J=\det(\mathbf{F})$ is the Jacobian of the deformation increment, and use was made of the symmetry of $\boldsymbol{\sigma}$. This equation can be linearized, which yields

$$\begin{aligned}&\int_{V_0}[(\mathbf{F}^{-1}\cdot d\boldsymbol{\sigma}+d\mathbf{F}^{-1}\cdot\boldsymbol{\sigma}):\delta\mathbf{F}J+(\mathbf{F}^{-1}\cdot\boldsymbol{\sigma}):\delta\mathbf{F}\,dJ]\,dV\\ &\quad=d\int_V \mathbf{q}\cdot\delta\mathbf{u}\,dV+d\int_S \mathbf{p}\cdot\delta\mathbf{u}\,dS\end{aligned} \qquad (12C.2)$$

Table 12.1 Difference between actual and approximate deformation rate in simple shear

γ	α
0.1	0.9996
0.2	0.9983
0.3	0.9963
0.4	0.9934
0.5	0.9899
0.6	0.9856
0.7	0.9806
0.8	0.9751
0.9	0.9690
1.0	0.9627

It is readily derived that $d\mathbf{F}^{-1} = -\mathbf{F}^{-1}\cdot d\mathbf{F}\cdot\mathbf{F}^{-1}$ and $dJ = J\,\mathrm{tr}(d\boldsymbol{\varepsilon})$, with $d\boldsymbol{\varepsilon}$ defined by Equation (12.21). Returning to the use of the current state as the reference state, it follows that

$$\int_V [(d\boldsymbol{\sigma} - d\mathbf{F}\cdot\mathbf{F}^{-1}\cdot\boldsymbol{\sigma}):(\delta\mathbf{F}\cdot\mathbf{F}^{-1}) + \mathrm{tr}(d\boldsymbol{\varepsilon})\boldsymbol{\sigma}:\delta\boldsymbol{\sigma}]\,dV$$

$$= d\int_V \mathbf{q}\cdot\delta\mathbf{u}\,dV + d\int_S \mathbf{p}\cdot\mathbf{u}\,dS \qquad (12C.3)$$

Now introduce the Jauman change in $\boldsymbol{\sigma}$,

$$d^J\boldsymbol{\sigma} = d\boldsymbol{\sigma} - \tfrac{1}{2}(d\mathbf{F}\cdot\mathbf{F}^{-1} - \mathbf{F}^{-T}\cdot d\mathbf{F}^T)\cdot\boldsymbol{\sigma} + \tfrac{1}{2}\boldsymbol{\sigma}\cdot(d\mathbf{F}\cdot\mathbf{F}^{-1} - \mathbf{F}^{-T}\cdot d\mathbf{F}^T) \qquad (12C.4)$$

With additional use of Equation (12.21), which may also be written as:

$$d\boldsymbol{\varepsilon} = \tfrac{1}{2}(d\mathbf{F}\cdot\mathbf{F}^{-1} + \mathbf{F}^{-T}\cdot d\mathbf{F}^T) \qquad (12C.5)$$

one can then transform Equation (12C.3) into,

$$\int_V [(d\boldsymbol{\sigma} - d\boldsymbol{\varepsilon}\cdot\boldsymbol{\sigma} - \boldsymbol{\sigma}\cdot d\boldsymbol{\varepsilon}):(\delta\mathbf{F}\cdot\mathbf{F}^{-1}) + (\boldsymbol{\sigma}\cdot\mathbf{F}^{-T}\cdot d\mathbf{F}^T):(\delta\mathbf{F}\cdot\mathbf{F}^{-1}) + \mathrm{tr}(d\boldsymbol{\varepsilon})\boldsymbol{\sigma}:\delta\boldsymbol{\varepsilon}]\,dV$$

$$= d\int_V \mathbf{q}\cdot\delta\mathbf{u}\,dV + d\int_S \mathbf{p}\cdot\delta\mathbf{u}\,dS \qquad (12C.6)$$

With use of various symmetries and the identity

$$\nabla\, d\mathbf{u} = \mathbf{F}^{-T}\cdot d\mathbf{F}^T$$

Equation (12C.6) transforms into

$$\int_V \{d^J\boldsymbol{\sigma}:\delta\boldsymbol{\varepsilon} - 2(d\boldsymbol{\varepsilon}\cdot\boldsymbol{\sigma}):\delta\boldsymbol{\varepsilon} + \mathrm{tr}(d\boldsymbol{\varepsilon})\boldsymbol{\sigma}:\delta\boldsymbol{\varepsilon} + \sigma:[(\nabla\, d\mathbf{u})\cdot(\nabla\, d\mathbf{u})^T]\}$$

$$= d\int_V \mathbf{q}\cdot\delta\mathbf{u}\,dV + d\int_S \mathbf{p}\cdot\delta\mathbf{u}\,dS \qquad (12C.7)$$

which is the desired linearized variational form.

REFERENCES

1. Zienkiewicz, O. C., and Godbole, P. N., 'Flow of plastic and visco-plastics solids with special reference to extrusion and forming processes, *Int. J. Num. Meth. Eng.*, **8**, 3 (1974).
2. Zienkiewicz, O. C., Jain, P. C., and Onate, E., 'Flow of solids during forming and extrusion: Some aspects of numerical solutions', *Int. J. Solids and Structures*, **14**, 15 1978).
3. McMeeking, R. M., and Rice, R. J., 'Finite element formulations for problems of large elastic–plastic deformation', *Int. J. Solids and Structures.*, **11**, 601 (1975).

4. Shimazeki, Y., and Thompson, E.G., 'Elasto-viscoplastic flow with special attention to boundary conditions', *Int. J. Num. Meth. Engrg*, **17**, 97 (1981).
5. Nagtegaal, J. C., and De Jong, J. E., 'Some computational aspects of elastic–plastic large strain analysis', *Int. J. Num. Meth. Eng.*, **17**, 15 (1981).
6. Hughes, T. J. R., and Lin, W. K., 'Nonlinear finite element analysis of shells: Part I—Three-dimensional shells, to appear in *Comp. Mech. Appl. Mech. Eng.* (1982).
7. Nagtegaal, J. C., 'On the implementation of inelastic constitutive equations with special reference to large deformation problems', presented at Fenomech II, stuttgart, 1981, to appear in *Comp. Meth. Appl. Mech. Eng.*
8. Hill, R., 'Some basic principles in the mechanics of solids without a natural time', *J. Mech. Phys. of Solids*, **20**, 111 (1972).
9. Krieg, R. D., and Krieg, D. B., 'Accuracies of numerical solution methods for the elastic–perfectly plastic model, *J. Pres. Vess. Tech.*, 1 (1977).
10. *MARC Programmers and Users Manual, Rev. J.*, MARC Analysis research Corporation, Palo Alto, California.
11. Lee, E. H., Mallett, R. L., and Yang, W. H., 'Stress and deformation analysis of the metal extrusion process', *Comp. Meth. in Appl. Mech. Eng.*, **10**, 339 (1977).
12. Lee, E. H., Mallett, R. L., and McMeeking, R. M., 'Stress and deformation analysis of metal forming processes', *Numerical Modeling of Manufacturing Processes, PVP-PB-025* (Eds James, R. F., Jr., Armen, H., and Fong, J. T.), ASME, 19 (1977).
13. Wertheimer, T. B., 'Problems in large deformation elasto-plastic analysis using the finite element method', PhD thesis, Stanford University, Palo Alto, California, to appear (1982).